Slot-Coupled Six-Element Sequential-Phase Circular Array for Directive Circular Polarization in L-Band

Gorka Casasus-Goyeneche, Miguel Ferrando-Rocher, Javier Vera-Sánchez, Miguel Ferrando-Bataller
Antennas and Propagation Lab, iTEAM Research Institute, Universitat Politècnica de Valencia (UPV), Spain
jcasgoy@upv.es

***Abstract*—This paper presents a six-element circular L-band array that uses sequential rotation, with a specifically designed feeding network and slot-coupled excitation. The microstrip feed network on Rogers RO4003C employs a two-stage division: a 1-to-2 split with a 180° phase shift, followed by two 1-to-3 dividers producing progressive phases (0°, 60°, 120°, 180°, 240° and 300°). Elements are excited through ground-plane apertures, and a low-permittivity foam spacer separates the feed and radiating layers to enhance efficiency. Full-wave simulations around 1.15 GHz demonstrate a good reflection coefficient with an impedance bandwidth exceeding 10%, a realized gain above 13 dBi, and circular polarization in the main beam from 1100 to 1180 MHz.**

***Index Terms*—Circular array, sequential rotation, slot-coupled antenna, microstrip feerding network, circular polarization, L-band, aperture coupling.**

I. Introduction

SATELLITE-enabled aviation services are moving from concept to in-orbit validation, pushed by an operational requirement that is very concrete, providing communications and surveillance over oceanic and remote regions where terrestrial infrastructure is unavailable or uneconomical. This evolution is happening under Air Traffic Management (ATM) constraints on safety, capacity, and efficiency, and with a clear pressure to modernize connectivity beyond incremental improvements [1]. In Europe, Startical (ENAIRE/Indra) is a representative example of this trend, with in-orbit demonstrators and public milestones associated with satellite-based aeronautical communications [2]–[4]. In the same direction, ESA's Iris programme targets satellite air–ground communications aligned with SESAR needs and aviation integration [5], [6]. Recent work also frames space-based VHF as a bridge technology toward future ATM connectivity, emphasizing progressive validation steps from trials to scalable services [7]. In parallel, space-based ADS-B has demonstrated the practical value of satellite reception for wide-area aircraft surveillance, motivating robust L-band reception front-ends in aviation-oriented payloads and terminals [8].

From an antenna standpoint, L-band terminals face a difficult balancing act as wavelength drives size, while platform constraints demand compactness, low mass, and manufacturability. Directive gain is typically obtained through arraying, but polarization robustness is equally critical. Sequential phase techniques have long been recognized as effective ways to obtain circular polarization (CP) and improve axial-ratio stability at array level without per-element quadrature feeding [9]–[11].

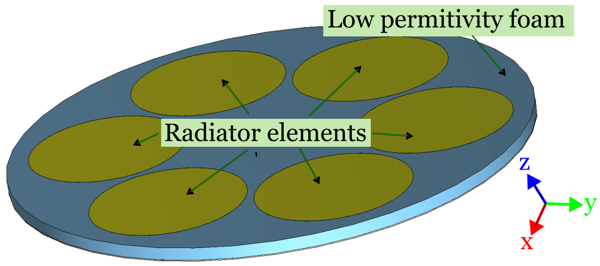

(a) Upper layer.

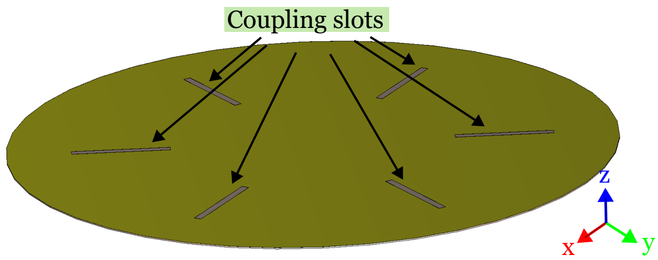

(b) Common ground plane.

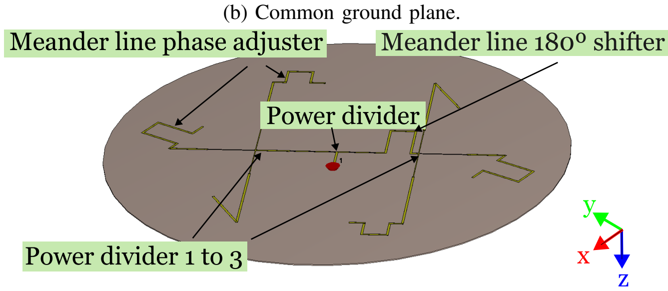

(c) Lower layer.

Fig. 1. Geometry of the antenna array.

This paper proposes a compact L-band six-element circular array that combines (i) a deterministic sequential-phase feeding network implemented in microstrip technology on Rogers RO4003C and (ii) slot-coupled excitation through apertures etched in the ground plane. A low-permittivity foam spacer ($\varepsilon_r \approx 1$) separates feed and radiating layers to reduce dielectric loading and enable a lightweight stacked implementation.

II. Antenna Description

The proposed antenna is a stacked, slot-coupled six-element circular array composed of two layers: an upper layer hosting

TABLE I
KEY DESIGN PARAMETERS OF THE PROPOSED L-BAND SIX-ELEMENT SEQUENTIAL-PHASE CIRCULAR ARRAY.

Parameter	Symbol	Value / Notes
Operating frequency (design)	f_0	1150 MHz
Overall diameter	D_{ant}	403.36 mm
Total height (stack-up)	H_{tot}	11 mm
RO4003C thickness	h_{sub}	0.831 mm
RO4003C relative permittivity	$\varepsilon_{r,\text{sub}}$	3.55
Copper thickness	t_{Cu}	35 μm
Foam thickness	h_{foam}	10 mm
Foam relative permittivity	$\varepsilon_{r,\text{foam}}$	1.06
Array ring radius (element centers)	R_{ring}	126.05 mm ($\approx \lambda/2$)
Number of elements	N	6
Element angular spacing	$\Delta\phi$	60°
Radiator diameter	D_{rad}	59.8 mm
Radiator-to-radiator edge spacing	g_{rad}	126.05 mm ($\approx \lambda/2$)
Slot length	L_{slot}	65 mm
Slot width	W_{slot}	5 mm
Slot orientation / rotation	–	90°
Feed input line impedance	Z_0	50 Ω
Main microstrip width (50 Ω)	W_{50}	1.85
Meander extra length 1	ΔL_{ph1}	20 mm
Meander extra length 2	ΔL_{ph2}	37.35 mm
Meander extra length 3	ΔL_{ph3}	20.15 mm

the radiating elements and a lower layer containing the feeding network, as illustrated in Fig. 1. Both layers share a common ground plane where six coupling slots are etched. The feeding network is implemented on Rogers RO4003C and separated from the radiating layer by a low-permittivity foam spacer. The radiating aperture consists of six identical circular elements uniformly spaced by 60° on a ring and excited through the ground-plane slots, which provide feed isolation, suppress spurious radiation, and offer additional tuning capability.

The feeding network delivers equal amplitudes and a uniform progressive phase around the array using a two-stage division. A 1-to-2 split creates two branches with a 180° phase difference, each feeding a 1-to-3 divider that generates the phase sets $0°, 60°, 120°$ and $180°, 240°, 300°$. The required phase shifts are realized through controlled microstrip line-length differences, including meandered sections: ΔL_{ph1} produces the 180° offset between branches, ΔL_{ph2} introduces a 60° shift between the first and second outputs, and an additional ΔL_{ph3} adds another 60° relative to the second branch. Replication of this structure on both branches yields the desired sequential rotation without active components, ensuring manufacturability and stable performance.

Key geometrical parameters of the stack-up were co-optimized via full-wave simulations to achieve good impedance matching over the operating band and circular polarization in the main-beam region.

III. Simulated Results

Full-wave simulations were performed for the complete stacked antenna. The input matching is shown in Fig. 2, a resonance appears near 1150 MHz, with $S_{11} \approx -15.5$ dB and the return loss remains below -10 dB between 1080 and 1200 MHz, giving a fractional bandwidth slightly above 10%.

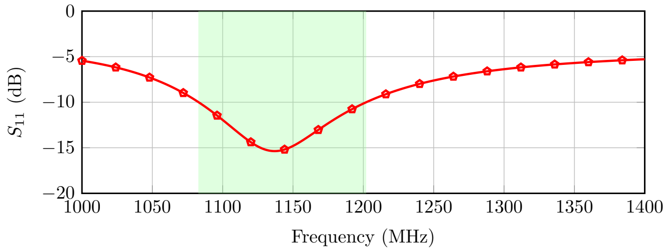

Fig. 2. Simulated input reflection coefficient magnitude (S_{11}).

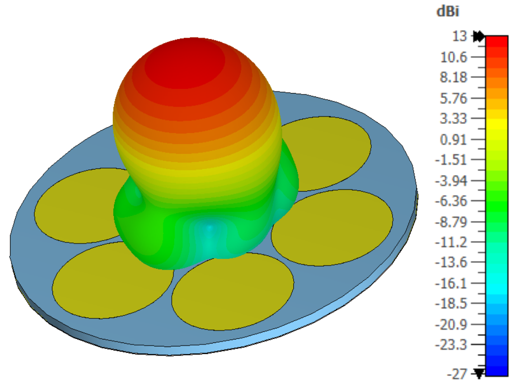

Fig. 3. Simulated 3D realized-gain pattern around 1.15 GHz. A single dominant main lobe is obtained, with peak realized gain close to 14 dBi.

Radiation performance at the design frequency is summarized in Fig. 3. The 3D realized-gain pattern shows a single dominant broadside main lobe, confirming coherent directive radiation from the array. The peak realized gain is 13 dBi, as indicated by the color scale. Which is consistent with expectations for a compact L-band array.

The axial ratio at the operating frequency for different ϕ cuts is shown in Fig. 4, confirming that the main-beam direction exhibits circular polarization. In addition, a frequency sweep was performed to assess the evolution of the axial ratio across the band (Fig. 5). The antenna maintains an axial ratio below 3 dB between 1100 MHz and 1180 MHz, resulting in a circular-polarization bandwidth of approximately 7%.

The normalized patterns for $\phi = 0°$ and $\phi = 90°$ are broadly consistent with each other, as expected from the circular and symmetric layout of the radiating layer (Fig. 6). The main beam is centered at $\theta = 0°$, sidelobes are well below the peak (down to -30 dB), and cross-polarization is around 20 dB below the copolar response, confirming good polarization purity.

Overall, simulations validate the architecture's directive broadside radiation, practical input matching, and circular polarization using a single-input, manufacturable corporate feed with slot coupling.

IV. Conclusion

This paper has presented a compact L-band six-element array. Circular polarization is achieved through a sequential-

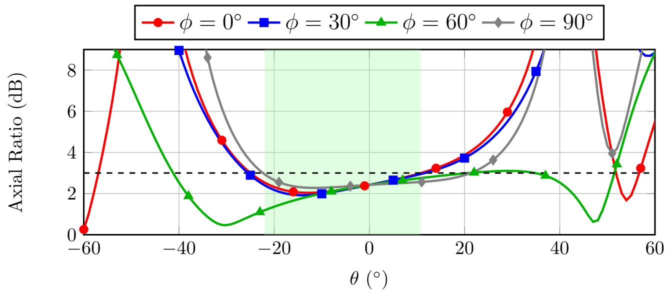

Fig. 4. Simulated axial ratio as a function of θ for several azimuth cuts ($\phi = 0°, 30°, 60°$, and $90°$).

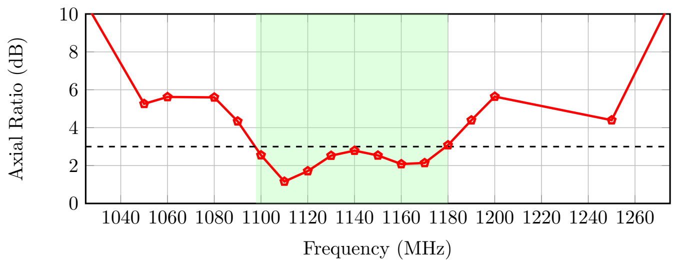

Fig. 5. Simulated axial ratio as a function of θ for several azimuth cuts ($\phi = 0°, 30°, 60°$, and $90°$).

rotation scheme, for which a microstrip feeding network has been designed and coupled to the radiating elements through ground-plane slots. The feeding network is implemented on Rogers RO4003C and distributes the required excitation phases to each radiating element using a two-stage power-division scheme, while a low-permittivity foam spacer separates the feed from the radiating layer to minimize dielectric loading.

Full-wave simulations indicate that the proposed stacked architecture can achieve a good input match around the design frequency, a directive main beam with realized gain above 13 dBi at 1.15 GHz, and circular-polarization behavior in the main-beam region enabled by the sequential-phase excitation. The results suggest that the combination of slot coupling and a deterministic corporate feed is a practical route to obtain directivity and polarization control with a single-input, manufacturable layout.

Future work will consist in the fabrication of a prototype to validate the simulated results and to assess the actual performance of the proposed design. To this end, a dedicated sensitivity study will be carried out to quantify the impact of the most critical manufacturing tolerances, particularly those associated with the feeding network, such as line dimensions, slot geometry, and layer alignment.

Acknowledgment

This work was supported by the SESAR 3 Joint Undertaking (SATERA Project, Grant Agreement No. 101164313), by the Spanish Ministerio de Ciencia e Innovación through projects PID2022-136869NB-C33 and PID2022-141055NB-C21, and by INDRA Espacio S.L.U. via the LINCE project within

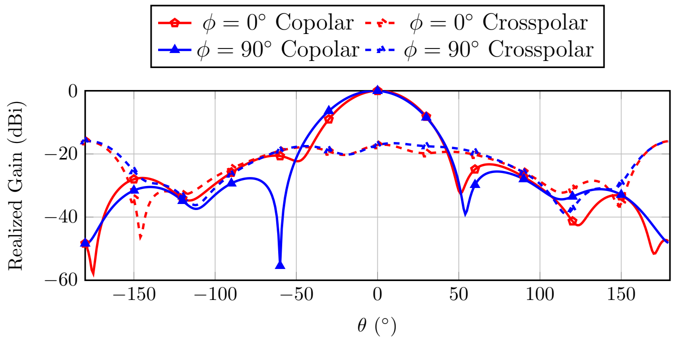

Fig. 6. Normalized radiation cuts around 1.15 GHz for $\phi = 0°$ (red) and $\phi = 90°$ (blue), showing copolar (solid) and crosspolar (dashed) components.

the Spanish Space Technology Program. Gorka Casasus-Goyeneche also acknowledges support from the Universitat Politècnica de Valencia through a UPV FPI predoctoral contract linked to project PAID-01-25.

References

[1] D. Reay, "Better Air Traffic Management: A Flight of Fancy?" *Research-Technology Management*, vol. 67, no. 3, pp. 5–6, 2024.

[2] ENAIRE, "Startical Has Launched Its First Satellite, IOD-1," https://www.enaire.es/en_GB/2025_03_17/ndp_startical_has_launched_first_satellite_iod1, 2025, accessed: 2026-02-25.

[3] SESAR Joint Undertaking, "ECHOES project marks global milestone in satellite-based VHF communications," https://www.sesarju.eu/news/echoes-project-marks-global-milestone-satellite-based-vhf-communications, 2025, accessed: 2026-02-25.

[4] Indra Group, "Startical achieves first-ever VHF voice communication between pilot and air traffic controller via satellite," https://www.indragroup.com/en/noticia/startical-achieves-first-ever-vhf-voice-communication-pilot-air-traffic-controller-satellite, 2025, accessed: 2026-02-25.

[5] European Space Agency (ESA), "Iris for aviation," https://www.esa.int/Applications/Connectivity_and_Secure_Communications/Iris_for_aviation, 2025, accessed: 2026-02-25.

[6] ESA Connectivity and Secure Communications, "IRIS - Satellite Communication for Air Traffic Management," https://connectivity.esa.int/iris-satellite-communication-air-traffic-management, 2025, accessed: 2026-02-25.

[7] A. A. Hijosa, M. M. Martínez, J. L. C. García, M. G. Martín, J. M. G. Cano, and D. F. Fernandez, "Space-based VHF, a bridge to the future," in *2025 Integrated Communications, Navigation and Surveillance Conference (ICNS)*. IEEE, 2025, pp. 1–8.

[8] Aireon, "Space-Based ADS-B Global Air Traffic Surveillance," https://aireon.com/surveillance-aireon/, 2019, accessed: 2026-02-25.

[9] J. Huang, "A technique for an array to generate circular polarization with linearly polarized elements," *IEEE Transactions on Antennas and Propagation*, vol. 34, no. 9, pp. 1113–1124, 1986.

[10] H. K. Kan and R. Waterhouse, "A small CP-printed antenna using 120/spl deg/ sequential rotation," *IEEE Transactions on Antennas and Propagation*, vol. 50, no. 3, pp. 398–399, 2002.

[11] A. B. Smolders and U. Johannsen, "Axial ratio enhancement for circularly-polarized millimeter-wave phased-arrays using a sequential rotation technique," *IEEE Transactions on Antennas and Propagation*, vol. 59, no. 9, pp. 3465–3469, 2011.